

Droplet-Interfaced Microchip and Capillary Electrophoretic Separations

Xize Niu,^{*,†} Fiona Pereira,[‡] Joshua B. Edel,[§] and Andrew J. de Mello^{*,‡}

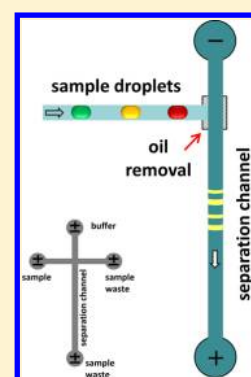
[†]Faculty of Engineering and the Environment and Institute for Life Sciences, University of Southampton, Highfield, Southampton, SO17 1BJ, United Kingdom

[‡]Department of Chemistry and Applied Biosciences, Institute for Chemical and Bioengineering, ETH Zürich, HCI E12S, Wolfgang Pauli Strasse 10, CH-8093 Zürich, Switzerland

[§]Department of Chemistry, Imperial College London, Exhibition Road, South Kensington, SW7 2AZ, United Kingdom

S Supporting Information

ABSTRACT: Both capillary and chip-based electrophoresis are powerful separation methods widely used for the separation of complex analytical mixtures in the fields of genomics, proteomics, metabolomics, and cellular analysis. However their utility as basic tools in high-throughput analysis and multidimensional separations has been hampered by inefficient or biased sample injection methods. Herein, we address this problem through the development of a simple separation platform that incorporates droplet-based microfluidic module for the encapsulation of analytes prior to the analytical separation. This method allows for the precise and reproducible injection of pL to nL volume isolated plugs into an electrophoretic separation channel. The developed platform is free from inter sample contamination, allows for small sample size, high-throughput analysis, and can provide quantitative analytical information.



Electrophoresis in all its embodiments is one of the most powerful and widely used tools in separation science and has been elaborated significantly since its introduction in 1937 by Arne.¹ For example, capillary gel electrophoresis (CGE) has played an essential role in genome sequencing² and 2D polyacrylamide gel electrophoresis is still considered the gold-standard in separating complex mixtures of proteins.³ In recent years, both capillary and chip based electrophoresis techniques have been used to provide for automated and high-throughput analysis in the fields of genomics, proteomics, metabolomics, enzyme analysis and cellomics.^{4–6} Such methods include capillary zone electrophoresis (CZE), capillary gel electrophoresis (CGE), micellar electrokinetic chromatography (MEKC), capillary isoelectric focusing (CIEF), and capillary isotachopheresis (CITP).⁷ Regardless of the embodiment, chip-based and capillary-based methods are notable for their ability to deal with small volumes, to provide for high separation efficiencies and component resolution and to be easily automated and coupled with downstream methodologies, such as liquid chromatography and mass spectrometry.⁸

While there have been extensive studies on separation conditions, surface chemistries and surface modifications,^{9,10} methods currently used for sample injection vary little from original formats proposed twenty years ago.^{11,12} Specifically, the two primary injection methods used in both capillary and chip-based electrophoresis are based on electrokinetic and hydrostatic injection.¹³ When using electrokinetic injection, biases arise at the injection point since analyte molecules have different electrophoretic mobilities. Accordingly, the absolute

number of injected molecules often does not reflect the analytical concentration in the original sample.² Hydrostatic injections are not biased in this manner, but conversely suffer from a lack of control when performed on-chip with respect to the volume delivered during the injection, and the overall throughput of the device. It should also be noted that although the injection zones in CE/MCE tend to be less than 10 nL, the actual sample needed for performing a separation is significantly higher. As a consequence, the majority of the sample is not analyzed, and thus traditional CE/MCE methods are not suited to the analysis of small samples without dilution.¹⁴ Indeed, operational modifications are often needed when, for example, performing electrophoretic single cell analysis.¹⁵

In recent years, droplet-based microfluidic systems have been increasingly popular due to a range of potential applications and performance advantages.^{16–20} Segmented flows formed within microfluidic channels have been shown to be powerful tools for encapsulating small molecules, biomolecules, cells and organisms into sub-nL volumes. To this end there have been a number of recent studies that have utilized droplets as a unique tool in transferring sub-nL volume samples to and from traditional capillary or microfluidic chips.^{21–24} Various methods have been developed to achieve precise and controllable

Received: May 7, 2013

Accepted: August 19, 2013

Published: August 19, 2013

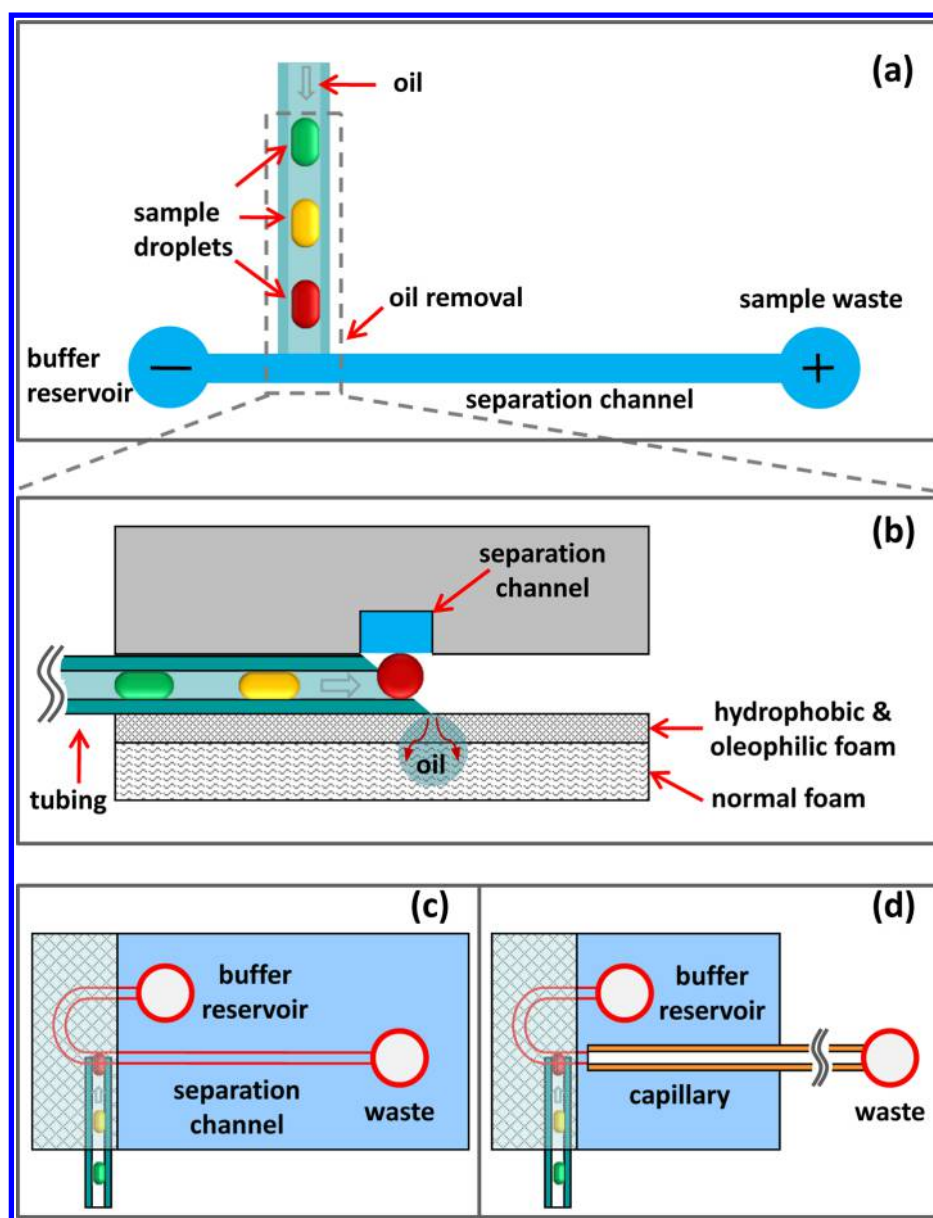


Figure 1. Schematic diagram of the microfluidic chip for droplet-interfaced electrophoresis separation. (a) The diagram of a general design illustrates the injection of sample droplets from a channel/tubing into a separation channel. (b) The side view of the magnified junction area showing oil removal and droplet injection into the continuous separation phase. (c) Top view of the microchip based CE system with PDMS separation channel. (d) Top view of the hybrid CE chip with capillary connected to the separation channel.

injections of droplets (to electrophoretic separation columns) in a reproducible manner. For example, sample droplets can be directly injected (using a carrier oil) into a separation channel,²³ or via hydrodynamic interactions,²⁴ or by surface treatments and controlled fusion of droplets into an electrophoresis sampling channel.^{25–27} Unfortunately, current approaches for removing the continuous phase to allow the release of droplet contents, are either complex, require precise pressure control within the fluidic channel, or necessitate the use of high electric fields.^{28–30} To this end, we recently demonstrated that incorporation of a hydrophobic and oleophilic membrane can be used for the efficient removal of carrier oil and immediate deposition of sample droplets onto a metal plate for matrix-assisted laser desorption/ionization and mass spectrometry analysis.³¹

Herein, we describe a novel method that allows the direct delivery of aqueous microdroplets into a separation channel by removing the oil phase within an open channel containing the hydrophobic and oleophilic membrane. The membrane is located at the junction between the “droplet channel” and downstream “separation channel” and allows the carrier oil to be absorbed passively into the membrane. This allows for the emergence of aqueous sample volumes into the separation channel without the introduction of flow instabilities, complex geometries or externally applied electrical fields. Importantly, this approach can be applied to both capillary and chip-based electrophoresis in free zone or gel formats, and can be used in a high-throughput and parallel manner. Furthermore, the method allows for the injection of pL-volumes of sample in a highly reproducible fashion. As the droplet/plug size is precisely

known, complete and quantitative electrophoretic separations can be performed with ease.

■ EXPERIMENTAL SECTION

Materials and Sample Preparation. Fluorescein 5(6) Isothiocyanate (FITC), Fluorescein and Eosin Y, Tris Borate EDTA (TBE), and polyvinylpyrrolidone (360 kDa MW) were obtained from Sigma (Dorset, U.K.). Polyethylene oxide (PEO, MW > 5 MDa) was obtained from Avocado Research Chemicals Ltd. (Lancashire, U.K.). All buffers were made using 18 M Ω deionized water (Purite, Oxford, U.K.) and filtered using 5 μ m pore membrane syringe filters (PALL Corporation, Hampshire, UK). Prior to use, the 1 \times TBE buffer was diluted 10 times with water and used in this form for all experiments. Henceforward, this diluted version of 1 \times TBE is referred to as TBE. Bare fused silica capillaries were obtained from Polymicrometer Technologies (Molex, Surrey U.K.). A 75 μ m internal diameter and 375 μ m outer diameter capillary was used for control experiments on a Peregrine HPCE instrument (deltaDOT, London, U.K.). Capillaries interfaced to the polydimethylsiloxane (PDMS) device had an internal diameter of 100 μ m and an outer diameter of 375 μ m.

FITC and Eosin Y were prepared at a stock concentration of 1.8 and 6 mg/mL, respectively, in water. Samples were further diluted 1000 times in TBE prior to droplet generation. The 50 bp dsDNA stepladder was obtained from Promega (Southampton, U.K.), while SYBR Green I was obtained from Invitrogen (Paisley, U.K.). A \times 500 stock of SYBR Green I was prepared in deionized water. The 50 bp ladder was diluted to 1/5 of the stock concentration in TBE and labeled with SYBR Green I at a final concentration of 1/100 of the stock concentration.

A 2.5% solution of polyethylene oxide (PEO) in TBE formed the electrophoresis sieving medium. The matrix was stirred for 24 h and then filtered and degassed prior to use. Polyvinylpyrrolidone (PVP) solution was prepared at a 10% w/w concentration in water and was used to coat the capillary to arrest EOF.

Microfluidic Chip Fabrication. Microchips were fabricated using conventional soft lithographic techniques.³² Briefly, SU-8 was photopatterned on a silicon wafer (IDB Technologies Ltd., North Somerset, U.K.) to form a master. After silanization, a PDMS mixture containing a 10:1 weight ratio for the base and curing agent (Dow Corning, Seneffe, Belgium) was poured on to the master and cured at 65 $^{\circ}$ C for 4 h to yield a 4 mm thick PDMS channel layer. The cured PDMS was subsequently peeled off the master and buffer and waste reservoirs were formed using a 4 mm biopsy punch (Nu-Care Products, Bedfordshire, U.K.). A 200 μ m thick bare PDMS layer was used as the bottom substrate. The two layers were aligned and bonded together, as shown in Figure 1C and D.

Capillary Preparation. Capillaries were cut to obtain a flat surface at the insertion end to the PDMS microdevice. The polyimide coating at this end was removed since it is not transparent and exhibits autofluorescence. A 2 cm detection window was created by burning the polyimide coating from the capillary. Prior to electrophoresis, capillaries were rinsed with methanol followed by deionized water. Capillaries were further cleaned with 0.1 M HCl, precoated with 10% PVP for 1 min and then loaded with the sieving matrix (2.5% PEO). Such cleaning and conditioning procedures were repeated after 50–60 droplet injections.

Microfluidic Chip Operation. Before use, chips were conditioned by rinsing the separation channel with 1 M NaOH or TBE. NaOH was used for separations employing electroosmotic flow, while 1 M HCL was used for the CGE separations without electroosmotic flow. This was followed by loading the separation channel with the electrophoresis buffer. Prior to sample analysis, a conductivity check was performed by applying increasing voltages across the separation channel. The polarity of the electric field was adjusted according to the direction of separation using a high voltage power supply (HVS448 3000 V, Labsmith, Livermore, U.S.A.).

Fluorescence Detection and Data Analysis. Fluorescence images were collected using a fluorescence microscope (Eclipse 400, Nikon, Surrey, U.K.) with a CCD camera (C4742-96, Hamamatsu Photonic Systems, Bridgewater, NJ). Briefly, light from a 100 W super high-pressure mercury lamp was passed through a FITC filter cube before being focused on the detection region of the chip or capillary using a 10 \times objective lens. Fluorescence emission was collected with the same objective and detected with the camera. *ImageJ* software was used to analyze recorded videos. Electropherograms were processed with Matlab (Mathworks).

Chip Design and Fabrication. Figure 1a shows a schematic of the droplet-based separation platform, which consists of a separation channel (6 cm long) and the droplet injection/loading tubing (Adtech, Stroud, U.K., i.d. 50–200 μ m and o.d. 400 μ m). The channel and the tubing join at a junction located 6 mm from the buffer reservoir. The separation channel is constructed in PDMS using conventional soft lithographic techniques by bonding a microstructured PDMS layer to a flat PDMS layer after plasma treatment of both surfaces. The formed separation channel is filled with either a buffer or sieving matrix for free-zone or gel electrophoresis, respectively. To perform the separation an electric field is applied between the buffer and sample waste reservoirs using platinum electrodes.

Process of Droplet Injection. The transfer of sample droplets from the delivery tubing into a separation channel occurs via an aperture at the tubing/channel junction. This aperture was created by removing a portion of PDMS from the bottom layer prior to plasma bonding. To ensure that the oil surrounding the analyte droplet is completely removed, a commercially sourced oleophilic foam was positioned near the injection junction. The foam consists of a hydrophobic and oleophilic PTFE membrane surface with a mesh size no greater than 5 μ m (Whatman, Cole–Parmer, London, U.K.). The foam is supported using a porous substrate made by stacking polyethylene sheets (Cole–Parmer, London, U.K.). The foam is highly efficient at absorbing hydrophobic oil and subsequently transporting it to the porous material underneath, while allowing the (previously enveloped) aqueous droplet to merge with the aqueous buffer in the separation channel. Importantly, it was found that when using a 10 mm \times 10 mm \times 1 mm piece of the stacked porous material covered with the foam, more than 200 μ L of the carrier oil (FC-40) could be absorbed before saturation. Within the current experimental setup, the oil/sample occupancy ratio is about 10:1 with an average droplet size of no more than 4 nL. Accordingly, 200 μ L of absorbed oil transfers a total sample volume of 20 μ L, which is equal to approximately 5000 droplets. In the unlikely scenario that sampling of more droplets is required, the foam can be regenerated or simply replaced.

A cross sectional schematic of the assembly is shown in Figure 1b. It should be noted, that the PTFE droplet delivery tube is cut at a 30° angle toward the separation channel. This ensures the spherical droplet coming out of the tubing can effectively contact the aqueous buffer in the separation channel. Since no surfactant is added to the continuous phase, whenever contact is made, droplets merge into the separation channel on a submillisecond time scale.³³ It should also be noted that in many droplet-based microfluidic systems surfactants are added to the carrier oil to stabilize droplets over extended time scales. This modification presents no significant difficulty to the current method, since electrodes can be directly incorporated with the injection tubing and a DC/AC voltage between the electrode and the nearest reservoir used to disrupt the surfactant and fuse the sample droplet into the separation channel.³⁰

In the experiments described herein, two platforms (Figure 1c and d) were used to accommodate both CZE and CGE separations. In Figure 1c, the channel is simply structured in PDMS. Such a design is suitable for CZE separations since the buffer can be easily filled from the reservoirs subsequent to plasma bonding. Conversely, when performing CGE with viscous sieving gels, the separation channel can be filled with separation buffer followed by the insertion of a fused silica capillary prefilled with gel (Figure 1d). In this respect, the channel contains a (300 × 150 μm cross section) expansion to facilitate insertion of the capillary. The primary difference between the CZE and the CGE device formats lies in the separation channel, with the injection parts being identical. During the sample injection process, a constant electrical field (the same as is used for the separation) is maintained throughout. Consequently separation of the molecules contained within the injected droplet occurs immediately after merging with the separation medium and without any alteration of the electric field. Significantly, the two-electrode configuration adopted simplifies substantially the optimization of separation conditions compared with standard cross channel-based MCE, where the optimal combination of injection voltage and injection time must be explored prior to any analysis.

RESULTS AND DISCUSSION

Droplet Injection. In initial studies, droplet injection was calibrated using the device shown in Figure 1c. Droplets had a volume of either 80 pL or 4 nL, contained 500 μM FITC in x 0.1 TBE buffer and were surrounded by an FC-40 oil phase. Droplets were pregenerated using an in-house droplet generation robot³⁴ and stored in PTFE tubing with an inner diameter of 50 or 100 μm. The relative standard deviation in droplet volume for both droplet sizes was calculated to be 8% (by analysis of over 600 droplets).

In the experiment, individual droplets were sequentially injected into the separation channel, as shown in the Supporting Information, with an electric field strength of 130 V/cm and an injection frequency of up to 5 droplets per second. Importantly, after a series of 100 injections (data not shown), no deposition or contamination of the fluorescence dye was observed at the injection point or in the PTFE tubing. Images of a droplet injection and the subsequent electrophoresis of droplet contents is provided in Figure 2a for an 80 pL droplet injected into a separation channel with a cross section of 50 × 50 μm. Figure 2b shows fluorescent signals for a

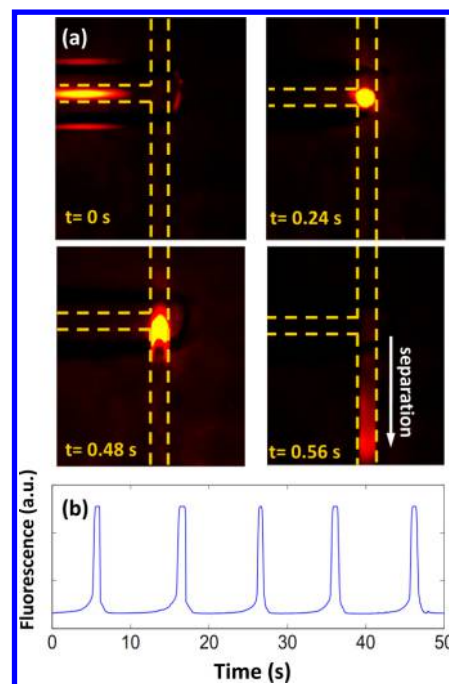


Figure 2. Droplet injection into the separation channel. (a) The snapshots of a 80 picolitre FITC droplet being injected from a PTFE tubing into the separation channel with a cross section of 50 × 50 μm². (b) Fluorescent signal shows injection of a sequence of droplets.

sequence of injected droplets (injections every 10 s), measured at the junction area.

It was found that for both tubing sizes, there is an optimal range of droplet sizes that can be reliably injected (Figure S2). For example, with 200 μm i.d. tubing, and a linear velocity of 50 μm/s, a droplet with a length less than 500 μm (15 nL in volume) can “jump” into the separation channel as a complete unit. Above this length, the droplet may break during the transfer process, leaving a satellite droplet in the delivery tube. Since the current setup utilizes 400 μm o.d. tubing (the smallest o.d. that could be accessed), the smallest droplet-volumes that are reliably injected have a volume of approximately 80 pL. The current injection volumes are slightly higher than would be encountered in chip-based electrophoresis with standard cross channels. Such a limitation can be removed in the future by replacing the PTFE tubing with thinner tubing or with microfabricated structures having small orifices.

An important feature of the current design is its ability to facilitate multiple injections of droplets into the separation channel, without accumulating separation buffer at the junction area. This feature relies on the local differential pressure defined by channel geometries. At the junction area, the buffer is confined within three solid walls, leaving an open surface. The curvature of the open surface can be either concave or convex, depending on whether the surface is below or above the channel walls (Figure S3). From Laplace’s law, the differential pressure across the liquid surface because of surface tension (ΔP_1) is inversely proportional to the radius of the curvature, $\Delta P_1 \propto \gamma / R_1$, where γ is the surface tension and R_1 the axial radius of the curvature along the channel direction. Such a pressure difference has a tendency to minimize the total surface area of the buffer. In the other words, if the buffer liquid is above the open surface (i.e., during sample droplet injection), pressure tends to push the liquid into the channel. When the liquid is below the surface (which can happen because of

evaporation), the pressure tends to pull supplementary liquid out. As shown in Figure 1a, the open channel at the junction area is located in the vicinity of one of the buffer reservoirs (6 mm) and the buffer liquid can flow between the junction and the buffer reservoir. Since the reservoir has an opening that is much larger than the channel width ($R_2 = 2$ mm for the reservoir while $R_1 = 25$ or 50 μm for the channel), the differential pressure at the liquid/gas interface in the reservoir ΔP_2 is confined to a very small value $\Delta P_2 \propto \gamma/R_2$, and is almost negligible compared to ΔP_1 at the junction during droplet injection. Therefore after droplet merging, the buffer is pushed from the junction to the buffer reservoir with a volume equal to the droplet size. This ensures multiple droplets can be injected sequentially into the separation channel.

Capillary Zone Electrophoresis. Capillary zone electrophoresis was performed within a PDMS microchannel as shown in Figure 1c. Separation channels were initially loaded with 1 M NaOH, which was replaced with a $\times 0.1$ TBE (pH 8.3) run buffer prior to separation. A conductivity check was performed to ensure stable electrical connection between the inlet and outlet reservoir (a more detailed assessment of current stability is provided in Supporting Information Figure S4), with an electric field being applied for 4 min to stabilize electroosmotic flow (EOF) in the channel. The flow rate for the droplet stream was set to 0.1 $\mu\text{L}/\text{min}$, resulting in a droplet injection interval of 35 s. Injected sample formed a discrete sample plug and migrated with the EOF downstream toward the detector.

Fluorescein iso-thiocyanate and eosin Y solutions at final concentrations of 100 and 500 μM , respectively, were prepared as a mixture in a $\times 0.1$ TBE buffer. (pH 8.3). At this pH both dyes are negatively charged and migrate behind the EOF. Separation was performed by applying a field strength of 266.6 V/cm between the buffer and waste reservoirs. Example electropherograms are shown in Figure 3. The percentage

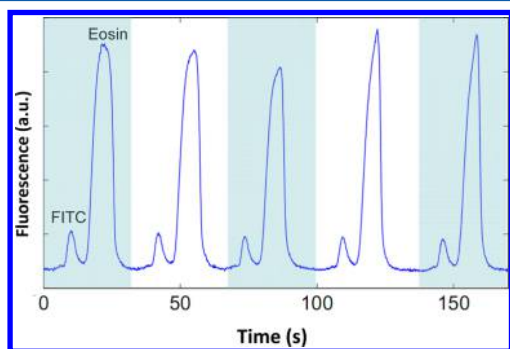


Figure 3. CZE separation of 5 consecutive droplets containing FITC and eosin Y. Conditions: field strength 100 V/cm, $\times 0.1$ TBE with pH 8.3, PDMS channel. FITC and eosin Y solutions at concentrations of 100 μM and 100 μM , respectively. Detection at 1 cm after the injection.

RSD values for the mobility of eosin Y and FITC over 30 injections were 7.9% and 8.9%, respectively, demonstrating excellent reproducibility. CZE is the most universal electrophoretic technique for the separation of a diversity of analytes including ions, small molecules, peptides, proteins, and carbohydrates.⁷ Alternate separation modes such as MEKC, CEC can provide enhanced separation under specific conditions, however these methods incorporate an identical sample loading process. Accordingly we expect that the

described droplet interface can be applied with minimal modification to these separation modes.

Capillary Gel Electrophoresis. Capillary gel electrophoresis is efficient in separating complex mixtures of nucleic acids and proteins through the use of polymer media, which contain selective physical barriers, such as polydimethylacrylamide, polyethylene oxide or dextran.³⁵ Such sieving media provide frictional forces that differentiate molecules by size or mass (rather than charge-to-mass ratio) and allow high-resolution separations of large biomolecules. Unfortunately, most sieving matrices are highly viscous, and loading the gel or sieving matrix into the channel requires application of higher pressures than encountered in CZE. In principle, this is unsuited to the droplet-interfaced channels described herein, which contain an open section. Moreover, the loading of the gel inside the channel cannot be easily monitored or controlled.

To solve the above challenges, a hybrid interface was adopted by connecting the PDMS chip to a fused silica capillary, as shown in Figure 1d. The droplet injection part was identical to that used in the CZE mode (Figure 1(c)), however the separation channel was shortened and replaced with a 300 μm wide channel to allow insertion of the capillary. The capillary employed has a 100 μm inner diameter and 375 μm outer diameter; is filled with 2.5% PEO gel in 8.9 mM Tris, 8.9 mM borate, and 0.2 M EDTA buffer after surface conditioning. The PDMS bottom layer under the outlet allows the capillary to be inserted smoothly and without chip delamination. Using the current buffer-gel format, there is no bulk flow in the capillary, since EOF is retarded by the PVP precoat and the high viscosity of the gel. During operation, any EOF in the open part of the channel will damage the connection, either through disconnection of the channel (if EOF is directed toward the nearest buffer reservoir) or by accumulation of buffer at the opening of the capillary if EOF is in the opposite direction. Accordingly, after chip bonding, the separation channel is filled with deionized water, which is then replaced with TBE buffer prior to operation. Such a process was found to effectively suppress the EOF.

A 50 bp dsDNA molecular weight standard was used to assess the performance of the droplet interface, as shown in Figure 4a. Fourteen out of sixteen fragments of this ladder could be unambiguously identified 11 mm from the point of injection. The sixteen fragments and the 1800 bp “backbone” fragment were separated within 55 s for each injection.

As a control, Figure 4c shows a capillary-based separation of the same ladder in a capillary with total length of 54 cm and an effective length 42 cm performed on the PEREGRINE I HPCE instrument (deltaDOT Ltd., U.K.). Figure 4d shows the separation of the same ladder in 2% agarose, provided by the manufacturer (Promega). Fragment molecular weights and assigned peak numbers are also provided. Figure 4b shows a plot of mobility versus fragment size for the separation shown in Figure 4(a) using the droplet interface. Data obtained for all three droplets follow the trend established for dsDNA ladders separated on other chip-based and macroscale CE systems. Each zone (I, II, III) marked in Figure 4b corresponds to a specific underlying sieving mechanism.³⁶ The lower molecular weight fragments undergo Ogston sieving (zone I), while the section of the curve showing an exponential decrease in mobility values corresponds to a reptation mechanism (zone II). Further along the curve biased reptation occurs, with dsDNA fragments aligning with the applied field and reducing the difference in mobility values (zone III).

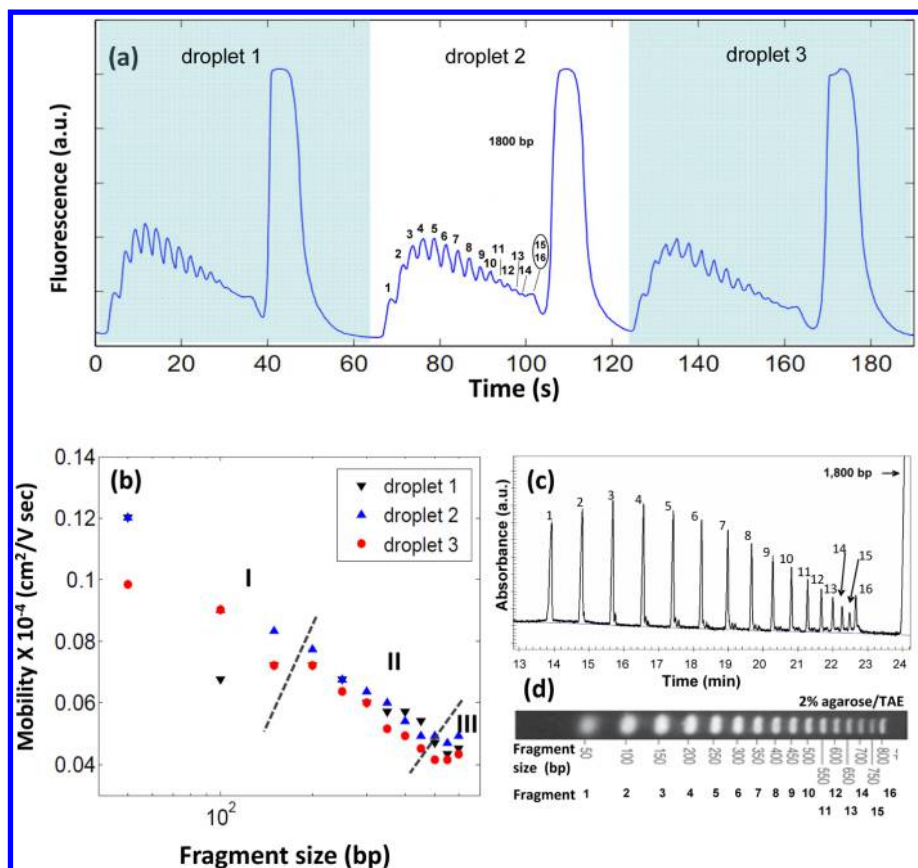


Figure 4. Multiple injection and separation of 50 bp dsDNA ladder (Promega, $0.034 \mu\text{g}/\mu\text{L}$) labeled with Sybr Green I ($50 \mu\text{g}/\text{mL}$). (a) Electrophoretic profile obtained for a multiple injection into a bare fused silica capillary. Detection was carried out ~ 1.1 cm from the point of injection. (b) Log–linear plot of fragment size versus mobility for the 3 consecutive injections in panel a. (c) Capillary separation of the same ladder (unlabeled) in a capillary with total length 54 cm and effective length 42 cm, performed using a PEREGRINE I label free intrinsic imaging CE instrument (deltaDOT, London, U.K.). Field strength, ~ 246 V/cm on droplet CE interface and ~ 203 V/cm on the CE instrument. 2.5% PEO in $\times 0.1$ TBE sieving matrix, the capillary was precoated with 10% PVP prior to loading with the sieving matrix. (d) The separation of the same ladder in 2% agarose as provided by the manufacturer (Promega). The band molecular weights and assigned peak numbers are also provided.

The multiple injection results presented in Figure 4 are only part of a larger group of sample droplets studied, with mobility values varying between 2% and 10%. A larger variation was observed for the smaller fragments, because of stretching of matrix pores by larger fragments from prior injections. Degradation of the sieving matrix is common to any multiple injection separation and thus the number of separations providing acceptable reproducibility needs to be established.

Quantitative Electrophoresis. Another key advantage of the described droplet CE interface is the ability to perform high-throughput injection of controlled volumes without bias. Accordingly, predefined sample volumes can be injected in their entirety, accurately reflecting the composition of the bulk sample. Accordingly, droplet CE separations has been demonstrated as a tool for quantitative analysis. This functionality is illustrated through the separation of a set of sample droplets that contain varying concentrations of fluorescein and eosin as shown in Figure 5a. Droplets were pregenerated with fluorescein concentration increasing from 6 to $15 \mu\text{M}$ but with eosin concentration decreasing from 74 to $18.5 \mu\text{M}$ in each set of 4 consecutive droplets. The fluorescein and eosin mixture produces two peaks when separated in a 2.5% PEO sieving matrix. The separation results obtained for two sets of droplets are shown in Figure 5b. Peak heights for fluorescein and eosin were determined for each droplet. Linear fitting of the curves generated by each analyte yielded R^2 values

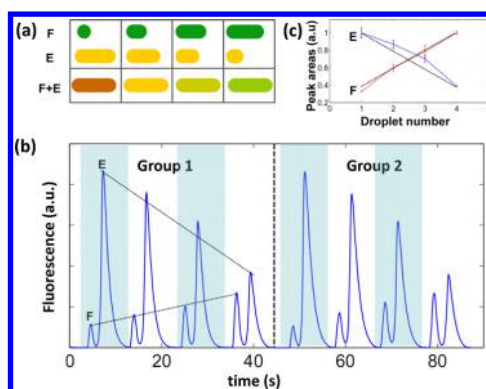


Figure 5. Screening on concentration conditions. (a) The droplets were pregenerated with fluorescein (F) concentration increasing from 6 to 9, 12, and $15 \mu\text{M}$ and eosin Y (E) decreasing from 74 to 55, 37, and $18.5 \mu\text{M}$ in every 4 consecutive droplets with 4% volume variation. (b) Electropherogram of two groups of droplets. (c) Comparison of experimental results (solid) with theoretical predictions (dashed).

in excess of 0.9, indicating excellent fits to the experimental data. Consequently, the signal obtained from each droplet accurately reflects its concentration, permitting the direct generation of calibration curves. Deviations from the fitted line are the result of small variations in droplet size and manual error during sample preparation. Figure 5 can also be analyzed

to extract the separation efficiency for the current system. At a detection distance of 1.5 cm, the theoretical plate number is about 7790. This value is 1 order of magnitude less than the glass chip-based separations.²⁶ The reduced plate numbers are likely to be a result of two factors. First, injection volumes in this experiment (4 nL) are relatively large when compared to typical volumes using standard crosspiece injectors, and second, separation conditions (such as gel/buffer concentration, surface coating, and electric field strength) have not been optimized.

CONCLUSIONS

Herein, we have demonstrated a droplet-interfaced CE platform for biological separations. The hybrid chip containing a hydrophobic and oleophilic film is shown to be effective in passive oil removal. Such a platform is simple to operate and can process small sample volumes. The system can operate in a high-throughput manner (>5 droplets per second), is free from cross-contamination between samples, and affords quantitative analysis in a direct manner. Both CZE and CGE separations have been successfully achieved, suggesting potential in a wide variety of applications such as small molecule separations, proteomics, genomics, metabolomics, and the other chemical and biochemical essays.

Significantly the droplet CE platform detaches droplet generation and handling from the process of electrophoretic separation. Accordingly, the vast majority of sample handling and preparation modules developed in droplet microfluidics (such as cell encapsulation and sample droplet collection from the other dimensional separations) can be hyphenated with the platform. The platform performs serial injection of droplets and is well suited to serial operations in droplet microfluidics and fast electrophoretic analysis. Moreover the passive handling approach developed here can be readily applied to a multiplexed system, with the potential for creating automated, multidimensional separations, without affecting the separation resolution.

ASSOCIATED CONTENT

Supporting Information

Additional material as described in the text. This material is available free of charge via the Internet at <http://pubs.acs.org>.

AUTHOR INFORMATION

Corresponding Authors

*Xize Niu: e-mail x.niu@soton.ac.uk.

*Andrew J. de Mello: andrew.demello@chem.ethz.ch.

Notes

The authors declare no competing financial interest.

ACKNOWLEDGMENTS

X.N. would like to thank the support from the EPSRC *Bridging the Gap* pilot project scheme (S11755102). A.J.d.M. would like to acknowledge partial support from ETH Zürich and the Global Research Laboratory Program of the National Research Foundation of Korea (Grant Number K20904000004-11A0500-00410). J.B.E. was partially funded by an ERC starting investigator grant and the EPSRC.

REFERENCES

- (1) Tiselius, A. *Trans. Faraday Soc.* **1937**, *33*, 524–531.
- (2) Huang, X. H. C.; Quesada, M. A.; Mathies, R. A. *Anal. Chem.* **1992**, *64*, 2149–2154.

- (3) Issaq, H. J.; Veenstra, T. D. *Biotechniques* **2008**, *44*, 697.
- (4) Dolnik, V.; Liu, S. R.; Jovanovich, S. *Electrophoresis* **2000**, *21*, 41–54.
- (5) Jorgenson, J. W.; Lukacs, K. D. *Science* **1983**, *222*, 266–272.
- (6) Kraly, J.; Fazal, M. A.; Schoenherr, R. M.; Bonn, R.; Harwood, M. M.; Turner, E.; Jones, M.; Dovichi, N. J. *Anal. Chem.* **2006**, *78*, 4097–4110.
- (7) Landers, J. P. *Handbook of Microchip Electrophoresis and Associated Microtechniques*; CRC Press: Boca Raton, FL, 2008.
- (8) Kolch, W.; Neuss, C.; Peizing, M.; Mischak, H. *Mass Spectrom. Rev.* **2005**, *24*, 959–977.
- (9) Breadmore, M. C. *J. Chromatogr. A* **2011**, *1221*, 42–55.
- (10) Breadmore, M. C. *Electrophoresis* **2007**, *28*, 254–281.
- (11) Harrison, D. J.; Manz, A.; Fan, Z. H.; Ludi, H.; Widmer, H. M. *Anal. Chem.* **1992**, *64*, 1926–1932.
- (12) Jacobson, S. C.; Hergenroder, R.; Koutny, L. B.; Warmack, R. J.; Ramsey, J. M. *Anal. Chem.* **1994**, *66*, 1107–1113.
- (13) Tabuchi, M.; Kuramitsu, Y.; Nakamura, K.; Baba, Y. *Anal. Chem.* **2003**, *75*, 3799–3805.
- (14) Berezovski, M.; Drabovich, A.; Krylova, S. M.; Musheev, M.; Okhonin, V.; Petrov, A.; Krylov, S. N. *J. Am. Chem. Soc.* **2005**, *127*, 3165–3171.
- (15) Gao, J.; Yin, X. F.; Fang, Z. L. *Lab Chip* **2004**, *4*, 47–52.
- (16) Huebner, A.; Sharma, S.; Srisa-Art, M.; Hollfelder, F.; Edel, J. B.; Demello, A. J. *Lab Chip* **2008**, *8*, 1244–1254.
- (17) Niu, X. Z.; de Mello, A. J. *Biochem. Soc. Trans.* **2012**, *40*, 615–623.
- (18) Solvas, X. C. I.; de Mello, A. *Chem. Commun.* **2011**, *47*, 1936–1942.
- (19) Song, H.; Chen, D. L.; Ismagilov, R. F. *Angew. Chem., Int. Ed.* **2006**, *45*, 7336–7356.
- (20) Utada, A. S.; Lorenceau, E.; Link, D. R.; Kaplan, P. D.; Stone, H. A.; Weitz, D. A. *Science* **2005**, *308*, 537–541.
- (21) Draper, M. C.; Niu, X. Z.; Cho, S.; Jarnes, D. I.; Edel, J. B. *Anal. Chem.* **2012**, *84*, 5801–5808.
- (22) Edgar, J. S.; Milne, G.; Zhao, Y. Q.; Pabbati, C. P.; Lim, D. S. W.; Chiu, D. T. *Angew. Chem., Int. Ed.* **2009**, *48*, 2719–2722.
- (23) Edgar, J. S.; Pabbati, C. P.; Lorenz, R. M.; He, M. Y.; Fiorini, G. S.; Chiu, D. T. *Anal. Chem.* **2006**, *78*, 6948–6954.
- (24) Niu, X. Z.; Zhang, B.; Marszalek, R. T.; Ces, O.; Edel, J. B.; Klug, D. R.; Demello, A. J. *Chem. Commun.* **2009**, 6159–6161.
- (25) Pei, J. A.; Nie, J.; Kennedy, R. T. *Anal. Chem.* **2010**, *82*, 9261–9267.
- (26) Roman, G. T.; Wang, M.; Shultz, K. N.; Jennings, C.; Kennedy, R. T. *Anal. Chem.* **2008**, *80*, 8231–8238.
- (27) Wang, M.; Roman, G. T.; Perry, M. L.; Kennedy, R. T. *Anal. Chem.* **2009**, *81*, 9072–9078.
- (28) Kelly, R. T.; Page, J. S.; Marginean, I.; Tang, K. Q.; Smith, R. D. *Angew. Chem., Int. Ed.* **2009**, *48*, 6832–6835.
- (29) Link, D. R.; Grasland-Mongrain, E.; Duri, A.; Sarrazin, F.; Cheng, Z. D.; Cristobal, G.; Marquez, M.; Weitz, D. A. *Angew. Chem., Int. Ed.* **2006**, *45*, 2556–2560.
- (30) Niu, X. Z.; Gielen, F.; de Mello, A. J.; Edel, J. B. *Anal. Chem.* **2009**, *81*, 7321–7325.
- (31) Pereira, F.; Niu, X.; deMello, A. J. *PloS One* **2013**, *8*, No. e63087.
- (32) Xia, Y. N.; Whitesides, G. M. *Annu. Rev. Mater. Sci.* **1998**, *28*, 153–184.
- (33) Niu, X.; Gulati, S.; Edel, J. B.; deMello, A. J. *Lab Chip* **2008**, *8*, 1837–1841.
- (34) Gielen, F.; van Vliet, L.; Koprowski, B. T.; Devenish, S. R. A.; Fischlechner, M.; Edel, J. B.; Niu, X. Z.; deMello, A. J.; Hollfelder, F. *Anal. Chem.* **2013**, *85*, 4761–4769.
- (35) Woolley, A. T.; Mathies, R. A. *Anal. Chem.* **1995**, *67*, 3676–3680.
- (36) Heller, C. *Electrophoresis* **2001**, *22*, 629–643.